Electronic Supplementary Material (ESI) for Sustainable Energy & Fuels.

Supporting Information

Integrated Catalytic Sequences for Catalytic Upgrading of Bio-derived Carboxylic Acids to Fuels, Lubricants and Chemical Feedstocks

Sankaranarayanapillai Shylesh[1,2], Amit A. Gokhale[1,3], Keyang Sun[2], Adam A. Grippo[1], Deepak Jadhav[1], Alice Yeh[1], Christopher R. Ho[2], Alexis T. Bell[1,2]*

[1]Energy Biosciences Institute, 2151 Berkeley Way, University of California, Berkeley, CA 94720, USA.

[2]Department of Chemical and Biomolecular Engineering, University of California, Berkeley, CA 94720, USA.

[3]BASF Corporation, 33 Wood Avenue South, Iselin, NJ, 07076, USA.

Materials and Methods

Materials: All chemicals were used as received without further purification. Commercially available carboxylic acids and fatty acids were purchased from Sigma-Aldrich, USA. All HPLC grade solvents, such as acetone, dichloromethane, diethyl ether, ethyl acetate, hexanes, and toluene were obtained from Fisher Scientific, USA. Anhydrous inorganic solids (Na_2CO_3, Na_2SO_4 and $MgSO_4$) were purchased from Fisher Scientific, USA. Catalysts and metal precursors such as zirconium nitrate hexahydrate, anatase titania, hydrotalcite and chloroplatinic acid hexahydrate were obtained from Sigma-Aldrich, USA.

Catalyst Preparation: Zirconia catalysts were prepared by the precipitation of zirconium nitrate hexahydrate (Aldrich, 99.99%) precursor at a high pH = ~13-14, using ammonium hydroxide as the precipitating agent. The precipitated mixture was stirred for another 30 minute and then at 353 K for 5 h. The mixture was then cooled to room temperature, filtered, washed with copious amounts of deionized water and dried at 373 K overnight. The dried solid sample was then calcined in air (100 cm^3min^{-1}) for 4 h at 823 K and 1023 K, respectively, for the synthesis of tetragonal (*t*-ZrO_2, BET_{SA}= 60 m^2g^{-1}) and monoclinic zirconia (*m*-ZrO_2. BET_{SA}= 49 m^2g^{-1}). Silica-supported tantalum oxide (Ta_2O_5) catalysts were prepared by an impregnation method using ethanol as a solvent. Corresponding amount of $TaCl_5$ dissolved in 10 mL ethanol were added dropwise to 5 g of silica support while grinding. The samples were dried at 383 K for 6 h followed by calcination at 773 K (2 ◦C/min) for 5 h. MgO doped Al_2O_3 catalyst, calcined hydrotalcite (Mg/Al=3) and hydroxyapatite (Ca-HAP, Ca/P=1.6) was prepared by the procedure reported by Shylesh, et al and Ho, et al[1,2].

Niobic acid and $NbOPO_4$ were received as a gift from CBMM, Brazil and was pretreated at 523 K and 823 K to yield Nb_2O_5 and $NbOPO_4$ catalyst. Supported Pt/$NbOPO_4$ was synthesized by an incipient wetness impregnation method using hexachloroplatinic acid (Aldrich) as the Pt precursor. In a typical synthesis procedure, 130 mg of H_2PtCl_6. $6H_2O$ dissolved in water was slowly added to 5.0 g of calcined $NbOPO_4$. After drying, the sample was then heated at 2 $^oCmin^{-1}$ to 573 K and reduced at this temperature in a hydrogen flow (50 $mlmin^{-1}$) for 3 h. TEM studies showed that the size of Pt particle deposited on $NbOPO_4$ support is ~ 8 nm.

Characterization: Metal content was determined by inductively coupled plasma optical emission spectroscopy (ICP-OES) conducted at Galbraith Laboratories (Knoxville, TN). Infrared spectra were acquired using a Thermo Scientific Nicolet 6700 FTIR spectrometer equipped with a liquid-nitrogen-cooled MCT detector. Each spectrum was obtained by averaging 32 scans taken with 1 cm^{-1} resolution. Approximately, 0.05 g of catalyst was pressed into a 20 mm-diameter pellet (<1 mm thick) and placed into a custom-built transmission cell equipped with CaF_2 windows, a K-type thermocouple for temperature control, and resistive cartridge heaters. Powder X-ray diffraction (PXRD) patterns were taken with a Bruker D8 GADDS diffractometer equipped with a Cu Kα source (40 kV, 40 mA). The specific surface area and pore size were calculated using the Brunauer-Emmet-Teller (BET) equation and Barrett-Joyner-Halenda (BJH) equations using a Micromeritics Gemini VII surface area and pore volume analyzer.

Reaction Studies: The gas-phase reaction of carboxylic acids to the internal ketones was performed in a 6.35 mm OD (~ 4 mm ID) quartz tube containing an expanded section (~12.7 mm OD, ~20 mm length). The reactor was packed with quartz wool above and below the catalyst bed to hold the catalyst in place. Carboxylic acids was injected into the He flow using a syringe pump. The catalysts were pretreated in He at 573 K for 1 h before being contacted with the feed. Experiments were carried out at 573 K, total gas pressures of 1 atm, and total gas flow rate of 100 cm^3min^{-1}. The carbon balance was found to be higher than 90% in all the experiments. Reaction products were analyzed using an Agilent 6890N gas chromatograph containing a bonded and cross-linked (5%-phenyl)-methyl polysiloxane capillary column (Agilent, HP-1) connected to a flame ionization detector.

Batch phase ketonic decarboxylation reactions were performed in a Parr autoclave apparatus. Typically, 3 mmol of the short chain carboxylic/fatty acid, 145 mg of nonane (internal standard), 7 mL of dodecane as solvent, 200 mg of the catalyst were added to the reactor and sealed. The reactor was purged with nitrogen, stirred and then heated to 553-593 K. After 5-6 h, the reactor was allowed to cool to room temperature and the catalyst was separated by centrifugation. The supernatant was diluted in dichloromethane

and the products were analysed by GC and GC-MS. Short chain C_2-C_4 carboxylic acids produce 10-20% of ketone condensation products and acid anhydrides over the ZrO_2 catalysts.

Condensation reaction of ketones were done as follows: 1-2 mmol of the ketone substrate, 145 mg of dodecane (internal standard), 3 mL of toluene was added to a 12 mL glass Q-tube reactor purchased from QLabtech. A polytetrafluroethylene (PTFE)-coated stir bar and 200 mg of the catalyst was then added to the reactor and was sealed with a PTFE coated silicone septum. The reactor was then immersed in a preheated oil bath at 453-523 K and stirred magnetically at 500 rpm for 18-24 h. After completion of the reaction, the Q-tube reactor was removed, cooled and the products were analysed by GC and GC-MS.

Hydrodeoxygenation reactions were carried out in eight unit HEL ChemSCAN autoclave system. In a typical experiment, 2 mmol of the internal ketone, 145 mg of nonane (internal standard), 3 mL of cyclohexane and 0.25 mol% $Pt/NbOPO_4$ was added to a HEL Hastelloy autoclave reactor. A PTFE coated stir bar was attached to the reactor and the autoclave was sealed. The reactor was purged three times with nitrogen and hydrogen prior to heating to the required reaction temperature. After stirring the reaction at 500 rpm for 4-6 h, the reactors were cooled to room temperature and the product mixture was centrifuged to separate the catalyst. Cracked products were observed in <10% in all cases. The supernatant was then diluted with dicholoromethane and the products were analysed by GC and GC-MS.

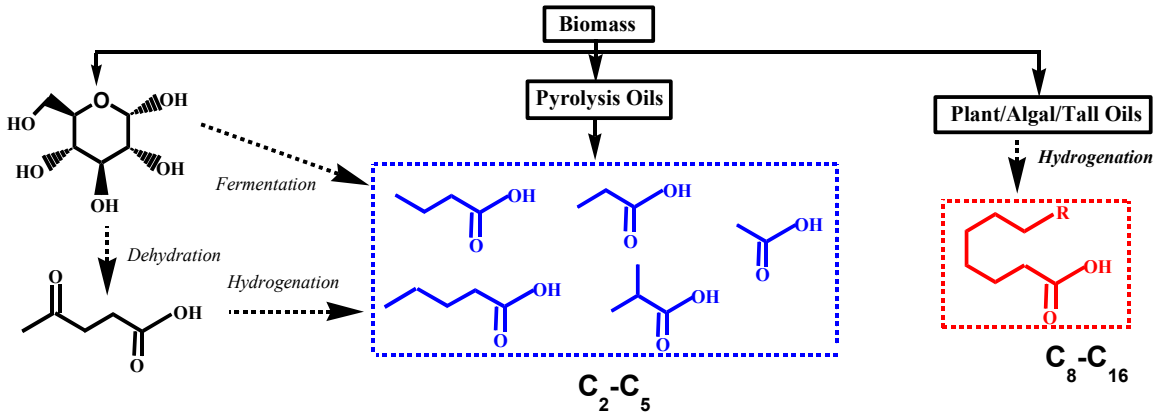

Scheme S1 Production of short chain and fatty acid from various bio-derived sources. Short chain C_2-C_5 carboxylic acids can be procured from pyrolysis oils and from fermentation pathways as shown in scheme. Pyrolysis-oils (bio-oils), for instance, produced from the fast pyrolysis of biomass, consist of highly oxygenated compounds and among oxygenates, light carboxylic acids (C_2-C_5) is one of the abundant single component in bio-oils. Short-chain carboxylic acids can also be produced by fermentation of biomass feedstocks and/or chemical pathways of sugars produced through biomass hydrolysis. Butyric acid, for example, can be generated in high titer (>60 gL^{-1}) from Clostridium tyrobutyricum by the anaerobic fermentation of glucose[3]. Valeric acid (pentanoic acid) can be chemically derived by the reduction of levulinic acid which inturn is produced through γ-valerolactone (GVL) produced by the hydrolysis of 5-hydroxymethylfurfural (HMF)[4]. Meanwhile, long chain fatty acids (C_8-C_{16}) can be produced from the hydrolysis of triglycerides or from various plant, animal, algal and tall oils[5]. Catalytic upgrading of these bio-derived light and fatty acids is thus an attractive route for replacing the fossil alternatives by renewable non-oxygenated 'drop-in' fuels and lubricants.

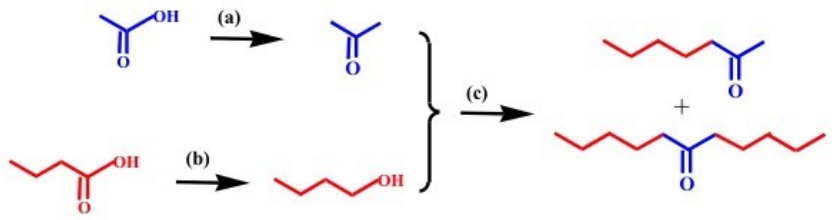

Scheme S2 Synthesis of methyl ketones and internal ketones from fermentation mixtures: (a) Ketonic decarboxylation of acetic acid to acetone over a ZrO_2 catalyst, (b) represent selective hydrogenation of carboxylic acids to the respective alcohols over a Ru-Sn/ZnO_2 catalysts[6] and (c) represent the mono and dialkylation of acetone and alcohols to the respective methyl and internal ketones over a Pd-Cu/HT catalyst[7].

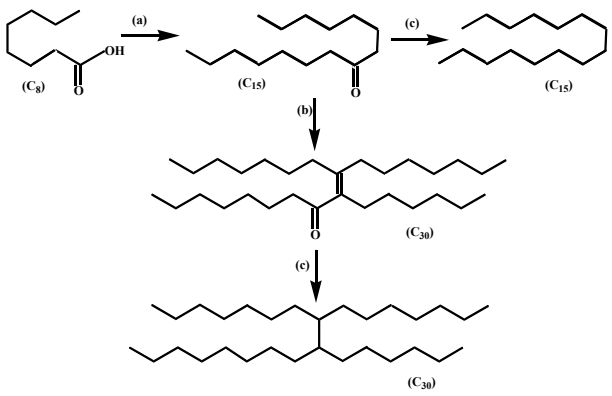

Scheme S3 Synthesis of diesel range C_{15} linear alkane and PAO type C_{30} alkanes from fatty acids. (a) Ketonic decarboxylation of C_8 fatty acid to the respective C_{15} internal ketone over a ZrO_2 catalyst, (b) dimerization reaction of C_{15} ketone to the respective C_{30} acyclic enone over a Nb_2O_5 catalyst, (c) represent $Pt/NbOPO_4$ catalysed hydrodeoxygenation of C_{15} internal ketone and C_{30} ayclic enones to the respective C_{15} linear alkane and C_{30} branched alkanes.

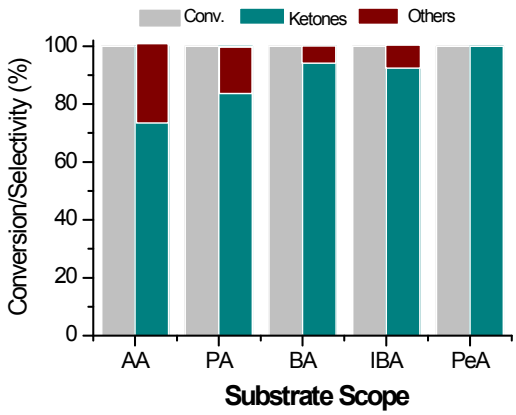

Figure S1. Ketonic decarboxylation of C_2-C_5 carboxylic acids in a Parr reactor to the respective ketones over ZrO_2 catalyst, where AA= acetic acid, PA = propanoic acid, BA = butyric acid, IBA = isobutric acid and PeA = pentanoic acid. Reaction Conditions: T = 573 K (553 K and 4 h is used for acetic acid substrate), Substrate Carboxylic Acid= 2 mmol, dodecane as solvent = 7 mL, t = 6 h, Mcat = 0.2 g. Others in the figure represent ketone condensed dimers, trimers and acid anhydrides; the formation of ketone condensed product decrease with an increase in carboxylic acid substrate chain length. In all instance, except with acetic acid, selectivity to the respective ketone product is >80%. For example, ketonic decarboxylation of acetic acid gives acetone, which subsequently undergoes aldol type condensation reactions giving mesitylene and isophorone as side-aldol products. Presumably, a combination of lower acidity of the alpha hydrogen on the C_2 carbon as well as the steric hindrance effects make the ketones derived from longer-chained acids stable under reaction conditions.[8]

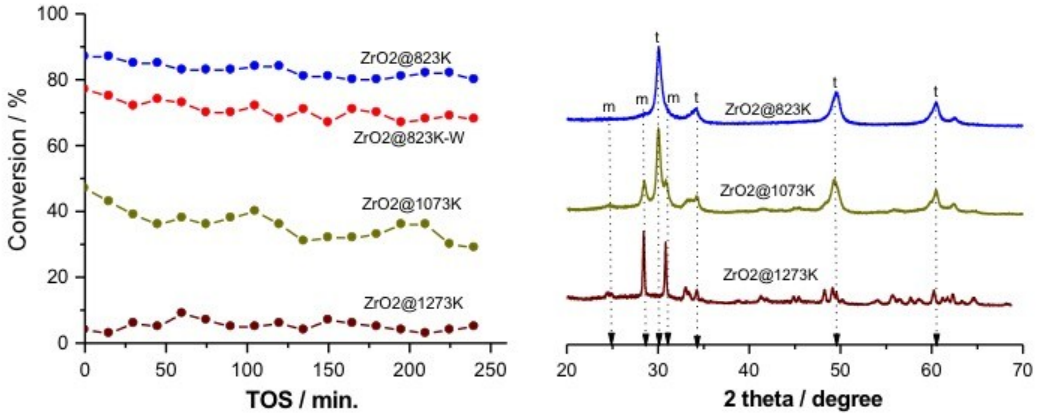

Figure S2. Ketonic decarboxylation of butyric acid to the respective internal ketone, heptan-4-one, over ZrO_2 pretreated at various temperatures. As fermentation mixtures and pyrolysis oils possess high water content (>50 %), water tolerance of the ketonic decarboxylation catalyst was also evaluated. ZrO_2@823K-W represent the activity of the ZrO_2@823K catalyst under 50wt.% water in the feed mixture, which showed no major differences in conversion or selectivity to the ketone products. Reaction Conditions: T = 573 K, WHSV = 0.6 h^{-1}, Q_{tot} = 100 $mLmin^{-1}$, Mcat = 0.1 g. Right side represent XRD patterns of ZrO_2 pretreated at various temperatures, where *t* represent tetragonal and *m* represent monoclinic zirconia phase.

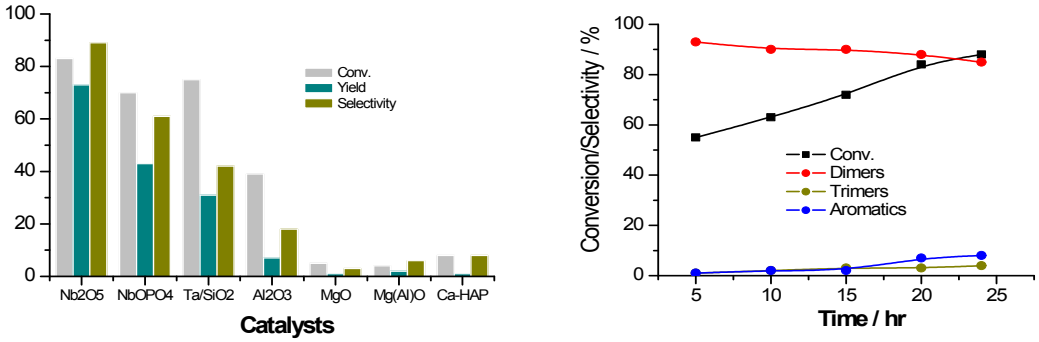

Figure S3. Selective dimerization reaction of heptan-4-one to the respective α,β unsaturated enones in a sealed Q-tube reactor over various acidic, basic and acid-base catalysts and time series plot of Nb_2O_5 catalyst in the condensation reaction of heptan-4-one. Reaction Conditions: T = 453 K, heptan-4-one = 2 mmol, toluene = 3 mL, t = 20 h, Mcat = 0.2 g. Nb_2O_5 catalyst retains similar catalytic results in presence of 10 wt.% of added water showing that these catalysts are water tolerant. Cyclic enone trimers and aromatic compounds constitute major side products with all catalysts screened.

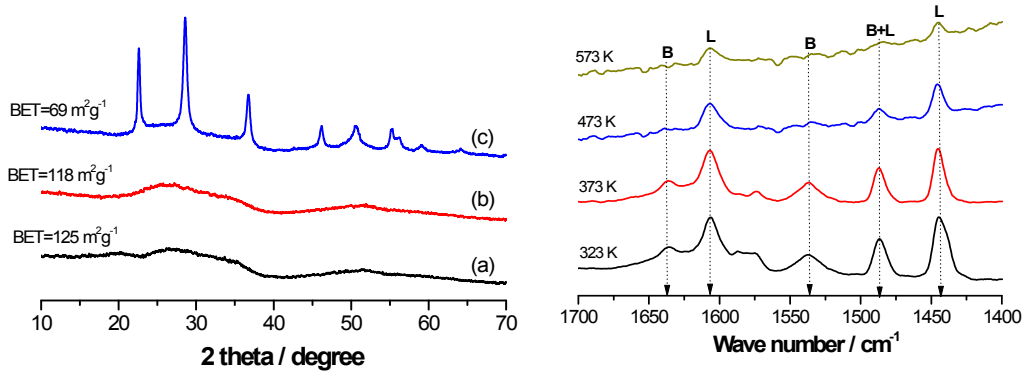

Figure S4. XRD patterns and BET surface area of Nb_2O_5 catalyst pretreated at different temperatures: (a) Nb_2O_5@373K, (b) Nb_2O_5@573K and (c) Nb_2O_5@773K . Pyridine IR studies showing the presence of Lewis acidic sites over the Nb_2O_5@573K catalyst; where, L stands for Lewis acid sites and B stands for Bronsted acid sites. The total acidity of Nb_2O_5@373K catalyst is 0.28 mmolg^{-1}, Nb_2O_5@573K is 0.20 mmolg^{-1} and Nb_2O_5@773K is 0.13 mmolg^{-1}.[9]

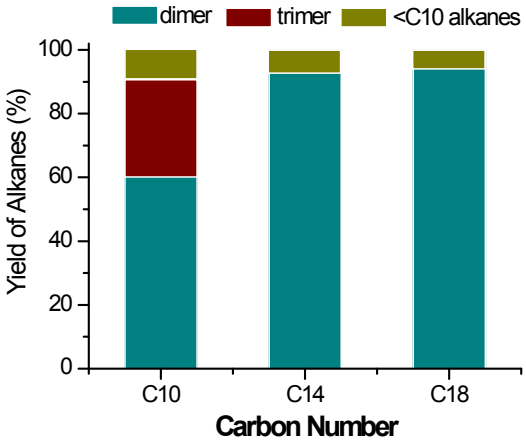

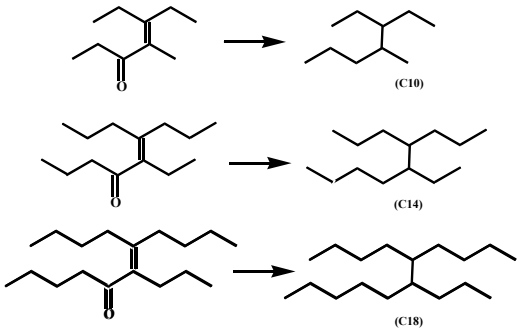

Figure S5. Hydrodeoxygenation of α,β-unsaturated enones produced from the ketonic decarboxylation-dimerization of pentan-3-one, heptan-4-one and nonan-5-one to the respective branched alkanes in a HEL reactor over the $Pt/NbOPO_4$ catalyst. Reaction Conditions: T = 453 K, IK = 2 mmol, cyclohexane = 3 mL, P_{H2} = ~3 MPa, MCat = 2.5 mol% Pt ($Pt/NbOPO_4$, Pt = ~1 wt.%), t = 6 h. <C10 alkanes represent lighter alkanes produced through cracking reactions. $Pt/NbOPO_4$ also retained its activity after three reaction cycles.

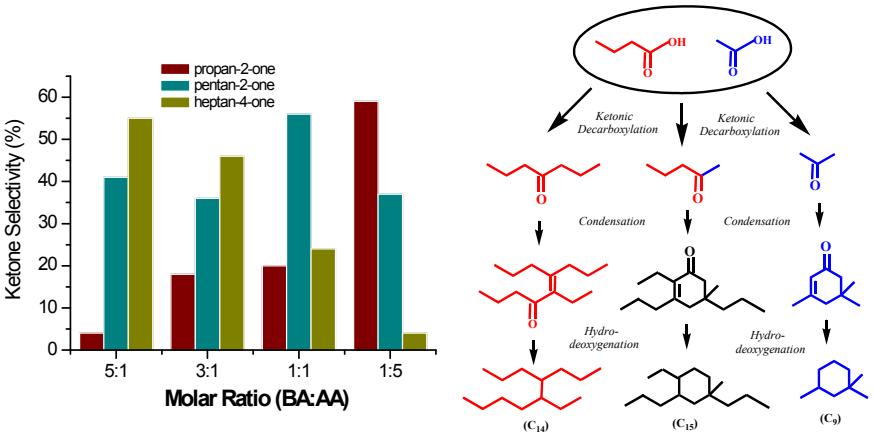

Figure S6. Cross-ketonic decarboxylation reaction of butyric acid (BA) and acetic acid (AA) under various molar ratios to the synthesis of internal ketones and methyl ketones over the ZrO_2 catalysts. Reaction Conditions: T = 573 K, Substrate Carboxylic Acids = 2 mmol, Solvent = 7 mL, t = 5 h, Mcat = 0.2 g. While alkyl methyl ketones can be catalytically trimerized to produce the cyclic enone condensates, internal ketones such as heptan-4-one exclusively produced the dimer condensates suggesting that the steric hindrance around the active center play an important role in tuning the products selectivity between the different class of ketone compounds produced by self- and cross-ketonic decarboxylation reactions.

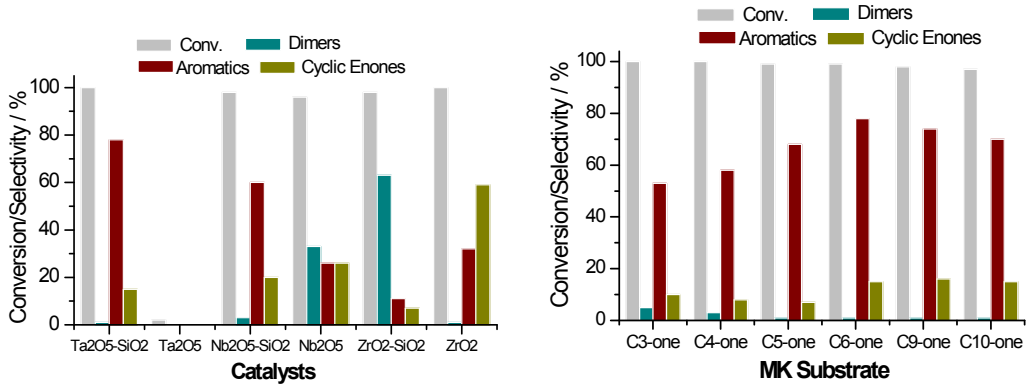

Figure S7. Condensation of hexan-2-one to alkylated aromatic compounds over various acidic catalysts. The alkylated aromatic compounds are mainly the 1,3,5 and 1,2,4 isomers. Reaction Conditions: T = 453 K, hexan-2-one = 2 mmol, t = 15 h, Solvent = 10 mL, Mcat = 0.2 g. Ta_2O_5/SiO_2 also retains similar catalytic results in presence of 10 wt.% of added water showing that these catalysts are water tolerant. Right side represents the activity of Ta_2O_5-SiO_2 catalysts in the condensation of C_3-C_{10} alkyl methyl ketones to the respective alkylated aromatic compounds. The C_{30} alkylated aromatics have excellent lubricant pour point (PP = -70 ^oC) and viscosity index (VI = 120) properties that are comparable to those of PAOs (PP = -72 ^oC and VI = 124).

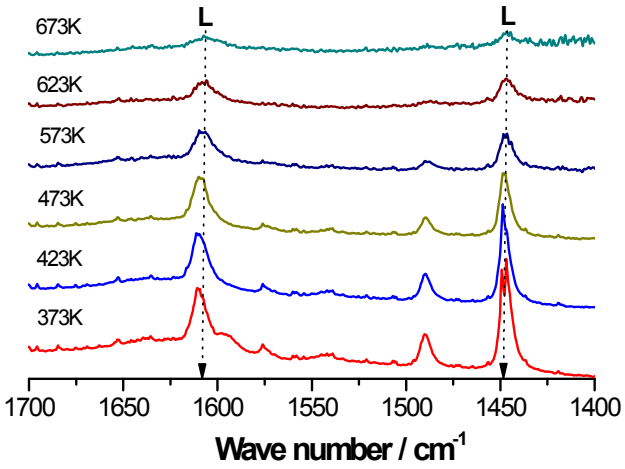

Figure S8. Pyridine IR studies showing the presence of Lewis acidic sites over the Ta_2O_5/SiO_2 catalyst at different desorption temperatures; where, L stands for Lewis acid sites at 1605 cm^{-1} and 1445 cm^{-1}.

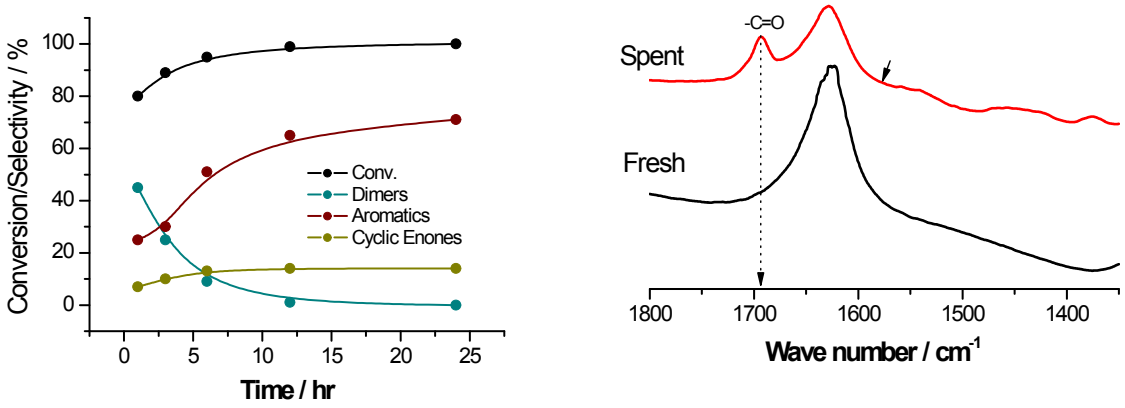

Figure S9. Reaction time profile of 2-hexanone conversion to aromatics and other compounds over a Ta/SiO_2 catalyst. Reaction conditions as shown in Table 1. In situ FT-IR spectra of Ta/SiO_2 catalyst before and after reactions. Spent catalysts showed the strong absorption of enones at ~1700 cm^{-1}, which relates to the less activity of the Ta/SiO_2 catalysts during reuse. Arrow represents the absence of poly aromatic compounds on the catalyst surface.

Table S1. Surface area and total acidity of condensation catalysts

Catalyst	BET Surface area (m^2g^{-1})	Total Acidity ($mmolg^{-1}$)[a]
ZrO_2	65 (62)	0.10
Nb_2O_5	118 (116)	0.28
$NbOPO_4$	140	0.32
Ta_2O_5/SiO_2	215 (208)	0.25

Values in parenthesis shows the surface area results after 10wt.% water co-feed experiments. [a]from ref [9-12].

References

1. Shylesh, S., Kim, S. D., Gokhale, A. A., Canlas, C. G., Struppe, J. O., Ho, C. R., Jadhav, D., Yeh, A. & Bell, A. T. Effect of composition and structure of Mg/Al oxides and their activity and selectivity for the condensation of methyl ketones. *Ind. Eng. Chem. Res*. **55**, 10635 (2016).

2. Ho, C., Shylesh, S. & Bell, A. T. Mechanism and kinetics of ethanol coupling to butanol over hydroxyapatite. *ACS Catal*. **6**, 939, (2016).

3. Zhu, Y., Wu, Z. & Yang, S. T. Butyric acid production from acid hydrolysate of corn fiber by Clostridium tyrobutyricum in a fibrous bed bioreactor. *Process Biochem*. **38**, 657 (2002).

4. Fitzpatrick, S. W. *US Patent* 4897497 (1998).

5. Smith, B., Greenwell, H. C. & Whiting, A. Catalytic upgrading of triglycerides and fatty acids to transport biofuels. *Energy Environ. Sci*. **2**, 262 (2009).

6. Lee, J-M., Upare, P. P., Chang, J-S., Hwang, Y. K., Lee, J. H., Hwang, D. W., Hong, D-Y., Lee, S. H., Jeong, M-G., Kim, Y. D. & Kwon, Y-U. Direct hydrogenation of biomass-derived butyric acid to n-butanol over a Ruthenium-Tin bimetallic catalyst. *ChemSusChem* **7**, 2998 (2014).

7. Goulas, K. A., Sreekumar, S., Song, Y., Kharidehal, P., Gunbas, G., Dietrich, P. J., Johnson, G. R., Wang, Y. C., Grippo, A. M., Grabow, L. C., Gokhale, A. A. & Toste, F. D. Synergestic effects in bimetallic palladium-copper catalyst improve selectivity in oxygenate coupling reactions. *J. Am. Chem. Soc*. **138**, 6805 (2016).

8. Baylor, R. A. L., Sun, J., Martin, K. J., Venkitasubramanian, P. & Wang, Y. Beyond ketonization: Selective conversion of carboxylic acids to olefins over balanced lewis acid-base pairs. *Chem. Commun*. **52**, 4975 (2016).

9. G. S. Nair, A. A. Alsalme, I. V. Kozhevnikov, D. J. Cooke, D. R. Brown and N. R. Shiju, *Catal. Sci. Technol*. **2**, 1173 (2012).

10. P. Wattanapaphawong, P. Reubroycharoen, A. Yamaguchi. *RSC Adv*. **7**, 18561 (2017).

11. Q-N. Xia, Q. Cuan, X-H. Liu, X-Q. Gong, G-Z. Lu, Y-Q. Wang. *Angew. Chem. Int. Ed*. **53**, 9755 (2014).
12. M. Baltes, A. Kytokui, B. M. Weckhuysen, R. A. Schoonheydt, P. Van der Voort, E. F. Vansant. *J. Phys. Chem. B* **105,** 6211 (2001).